Scattering layer statistics from space borne GLAS observations

F.M. Bréon, D. M. O'Brien, J. D. Spinhirne

Scattering layer statistics from space borne GLAS observations

F. M. Bréon,[1] D. M. O'Brien,[2] and J. D. Spinhirne[3]

Received 17 June 2005; revised 22 August 2005; accepted 26 September 2005; published 18 November 2005.

[1] Cloud and aerosol layers detected by the space borne Geoscience Laser Altimeter System (GLAS) are used to derive statistics of clear and almost clear atmospheres, the latter defined to be those with some scattering material but total optical thickness less than 0.2. Such statistics are needed to evaluate the potential coverage of NASA's forthcoming Orbital Carbon Observatory. The global fraction of clear cases is approximately 15%, with large scale spatial structures similar to those found by passive sensors. The spatial distribution of almost clear cases is similar to that for clear, with global fraction approximately 20%. The mean altitude of optically thin scattering layers is generally below one kilometer, indicating that they are composed mostly of boundary layer aerosol rather than high altitude cloud. The spatial correlation function of clear cases is accurately reproduced by the analytical function $F(d) = \exp[-(d/d_0)^{0.5}]$, where d_0 is a correlation scale length. Between 60N and 60S, d_0 shows little zonal variation, and its average value is 320 km. Over the Arctic d_0 falls to 250 km, but rises to 450 km over the Antarctic. **Citation:** Bréon, F. M., D. M. O'Brien, and J. D. Spinhirne (2005), Scattering layer statistics from space borne GLAS observations, *Geophys. Res. Lett.*, *32*, L22802, doi:10.1029/2005GL023825.

1. Introduction

[2] The Orbiting Carbon Observatory (OCO) [*Crisp et al.*, 2004] is designed to estimate the column averaged dry air mole fraction of carbon dioxide, denoted X_{CO2}, with sufficient accuracy to improve our knowledge of surface carbon fluxes. The instrument provides high spectral resolution Earth reflectance spectra in the oxygen A-band at 0.76 μm and two CO_2 absorption bands at 1.6 μm and 2 μm. In clear conditions, X_{CO2} can be estimated from the spectra using the technique of differential absorption. To correct for scattering and surface pressure effects, the estimated CO_2 column must be normalized by a similar estimate of the well-mixed O_2 column, derived from the 0.76 μm spectrum. There are significant uncertainties associated with this normalization, resulting from the spectral variation of the optical properties of the scattering layer between the O_2 and CO_2 bands and also from the coupling with the surface reflectance. The uncertainty increases with the optical thickness, and the threshold beyond which accurate measurements of X_{CO2} become impractical is not known precisely, but it is likely to be about 0.2. To assess the fraction of useful OCO soundings, statistics are needed in almost clear atmospheres of the spatial and vertical distributions of scattering material, the latter because the impact of a scattering layer on the spectra depends sensitively on its pressure altitude. Finally, the spatial distribution of clear cases is also needed, as the correlation scales of scattering layers and X_{CO2} are clearly different. While passive instruments such as MODIS can be used to assess the spatial distribution of clouds and aerosols, their sensitivity to the vertical distribution is poor, particularly so for the thin layers that are of interest here. In contrast, lidar provides both the vertical distribution of scattering material and an estimate of the total optical thickness, provided that the scattering layers are thin. The Geoscience Laser Altimeter System (GLAS) was launched in January 2003 on the NASA ICESAT satellite. Although planned for a 3–5 year life, on orbit laser reliability problems have limited observations to intermittent one to two month periods every three to four months [*Abshire et al.*, 2005]. In this paper, GLAS products for an eight week period from 2003-09-25 to 2003-11-18 are used to derive statistics relevant to OCO.

2. Data and Methods

[3] The analysis in this paper is based on GLAS product GLA11, release number 19 [*Zwally et al.*, 2004] (available at http://nsidc.org/data/docs/daac/glas_atmosphere/gla11_records.html), which reports cloud layers, derived from 40 Hz pulse profiles averaged over one second (spatial resolution 6.9 km along track), and aerosol layers at a resolution of 4 seconds (28 km along track). The GLAS data processing [*Palm et al.*, 2002] identifies layers using thresholds, gradients and other tests, and retrieves optical thickness from forward integration of the lidar signal combined with regional and height based aerosol scattering models. Experimental verification of initial measurements indicates that cloud and aerosol layers with backscatter cross sections down to 10^{-7} $m^{-1}sr^{-1}$ and optical thickness down to 0.01 generally were detectable for the fall 2003 operating period [*Spinhirne et al.*, 2005; *Hlavka et al.*, 2005]. Highly sensitive aircraft measurements in the Pacific basin indicated background tropospheric aerosol, with backscatter cross section $2–5 \times 10^{-9}$ $m^{-1}sr^{-1}$ at visible wavelengths, and inferred boundary layer aerosol optical thickness frequently less than 0.003 [*Menzies et al.*, 2002]. Thus, it is realistic that the aerosol and cloud optical thickness is less than 0.01 when GLAS does not detect a layer, and that such conditions exist for remote regions. As a consequence, in this paper we define as "clear" an atmosphere with an optical thickness less than 0.01.

[4] Quantities calculated were the optical thickness of aerosol, both from the boundary layer and elevated layers, and the optical thickness of cloud. For a given day and

[1]Laboratoire des Sciences du Climat et de l'Environnement, CEA/DSM/LSCE, Gif sur Yvette, France.
[2]Atmospheric Science Department, Colorado State University, Fort Collins, Colorado, USA.
[3]NASA Goddard Space Flight Center, Greenbelt, Maryland, USA.

0094-8276/05/2005GL023825

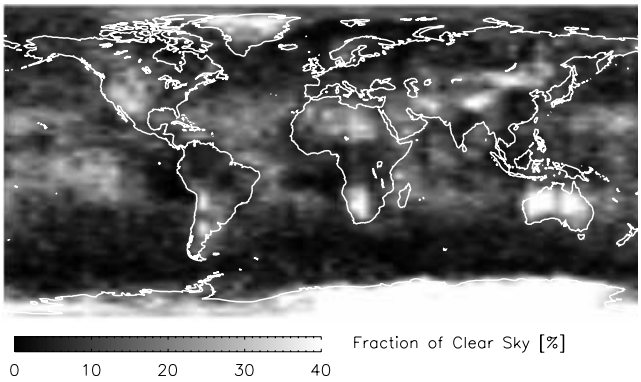

Figure 1. Fraction of totally clear sky with neither cloud nor aerosol detected from the GLAS vertical profiles.

location, the mean heights of aerosol and cloud were obtained by weighting the pressure height of each detected layer by its optical thickness. However, in the monthly means, daily heights were not weighted by the optical thickness. Four categories were extracted from the data:

[5] 1. totally clear sky (no aerosol or cloud detected by the algorithm);

[6] 2. no cloud but aerosol optical depth between zero (excluded) and a threshold;

[7] 3. no aerosol but cloud optical depth between zero (excluded) and a threshold;

[8] 4. total optical thickness of aerosol and cloud between zero (excluded) and a threshold. Category 4 includes categories 2 and 3. The threshold chosen for this analysis is 0.2, but similar results were obtained with 0.1.

[9] GLAS derives the optical thickness at the laser wavelength of 532 nm. In the OCO bands, the optical thickness of aerosol generally will be smaller, as optical thickness typically decreases with wavelength. However, the major scattering layers identified in the analysis (dust in the Sahara, boundary layer aerosol over the oceans) are composed of relatively large particles, whose spectral signatures are rather flat. For such large particles, the decrease in optical depth from 532 nm to the longer OCO band (2 μm) is expected to be by a factor less than 2.

3. Results

[10] Figure 1 shows the frequency of category 1 cases (totally clear sky), which globally averaged is approximately 15%. There are very strong spatial variations, both zonal and longitudinal. Clear cases are common over the deserts of both hemispheres, located over the downward branches of the Hadley cells. The clearest areas are found over the ice caps of Greenland and Antarctica, partly because these areas have very low amounts of aerosol. Regions with the lowest clear fractions are the mid-latitude storm tracks in both hemispheres, and regions of oceanic stratocumulus (east of the oceanic subtropical basins). Table 1 shows the zonal averages of the clear sky fraction, together with other statistics. It confirms that the clearest zonal bands are found around 25°, both north and south, and close to the poles. There is an asymmetry between the north and south polar regions, which may be due both to the different season and to the presence of the elevated Antarctic land mass. Overall, the cloud cover derived from GLAS agrees qualitatively with that from MODIS [*Hart et al.*, 2005].

[11] GLAS shows a large fraction of category 2 cases (thin aerosol but no cloud), the statistics of which are in Table 1. Of the cases without cloud, over half have a detectable aerosol layer, except at high latitudes, and their longitudinal distribution is similar to Figure 1. This indicates that the frequency of category 2 cases is mostly modulated by cloud cover. Over the oceans the mean height of aerosol layers is less than 1 km, without significant spatial structures, and the bulk of the optical thickness is in the boundary layer. In contrast, aerosol layers are observed several kilometers above land surfaces. For example, over the Sahara the mean height is about 2 km, while in southern Africa aerosol layers, most probably from biomass burning, reach an average height of 4 km. Significant seasonal variations are expected, caused by meteorological conditions that drive both convection and biomass burning. Because the currently processed GLAS dataset is limited in time, it does not permit further investigation of the seasonal variability.

[12] The frequency of category 3 cases (thin cloud but no aerosol) is lower than category 2 (Table 1). Maximum frequencies are approximately 10% in some areas of the tropics and high latitudes, but at mid-latitudes the frequency is low. These results indicate that the semi-transparent high-clouds frequently observed by passive sensors generally have optical thickness larger than our threshold. The thin cloud layers are much higher than the aerosol layers, being over 10 km in the tropics. Lower average heights are observed at mid-latitudes, but with a very low occurrence (a few %), so this result may not be statistically representative.

[13] Figure 2 shows the frequency of category 4 cases (almost clear). In a large fraction of the tropics, the

Table 1. Fraction [%] of Clear Areas and Spatial Scale d_0 for 10° Zonal Bands[a]

Latitude Band	Totally Clear	Thin Aerosol	Thin Cloud	Almost Clear	d_0[km]
80–90N	13.5	7.0	7.0	15.7	214
70–80N	10.6	5.2	5.4	12.0	276
60–70N	8.1	4.6	4.2	9.7	242
50–60N	8.4	7.6	3.0	11.8	359
40–50N	11.8	14.0	2.8	18.5	359
30–40N	13.9	18.5	3.5	23.6	345
20–30N	16.6	24.7	3.7	30.4	338
10–20N	14.0	19.6	6.3	30.0	338
Eq–10N	10.8	12.4	7.4	24.3	310
Eq–10S	11.6	15.9	6.4	26.8	331
10–20S	14.0	16.9	4.1	23.4	283
20–30S	16.1	18.3	2.8	22.4	297
30–40S	8.8	14.2	2.7	18.3	283
40–50S	5.2	6.9	2.2	9.8	317
50–60S	3.5	4.2	2.1	6.7	297
60–70S	10.4	4.4	3.2	8.1	455
70–80S	35.3	7.4	6.3	14.2	490
80–90S	43.8	8.9	5.2	14.5	448

[a]"Totally clear" refers to cases with neither aerosol nor cloud detected by GLAS. "Thin aerosol" refers to cases with a total aerosol optical thickness between 0 (excluded) and 0.2, but without cloud. "Thin cloud" is the same for cloud, but without aerosol. "Almost clear" refers to cases when the total optical thickness is between 0 (excluded) and 0.2. The correlation distance d_0 is the distance at which $F(d)$ takes the value 1/e.

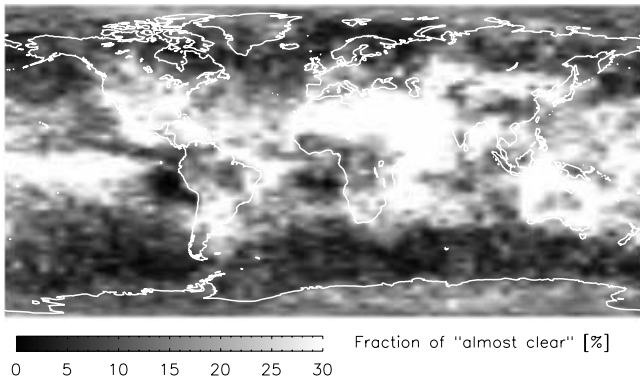

Figure 2. As for Figure 1, but for cases with scattering optical thickness, due to either cloud or aerosol, less than 0.2.

frequency exceeds 30%, and in the band from 40N to 40S almost clear atmospheres are about twice as numerous as totally clear (Table 1). Figure 3 shows the mean height of the scattering layer for the category 4 cases. There is a large contrast between convective areas of the tropics, where mean heights exceed 10 km, and oceanic areas of the tropics and mid-latitudes, where the mean height appears dominated by the presence of boundary layer aerosol. Other areas show intermediate values, most likely resulting from a mixture of high cloud and lower aerosol layers.

[14] The extent to which some areas have persistent thin scattering layers, while others remain clear, is addressed in Figure 4. The scatter plot of the clear and almost clear fractions shows that they are spatially correlated. This indicates that the availability of clear and almost clear situations, suitable for OCO processing, is modulated mostly by the presence of thick cloud, rather than by the distribution of aerosol. The branch of points with the clear fraction larger than the almost clear corresponds to Antarctica and Greenland. Elsewhere, Figure 4 demonstrates that thin scattering layers are more frequent than perfectly clear atmospheres.

[15] We now discuss the spatial correlation of clear areas. We consider only cloud, irrespective of the presence of aerosol, because the larger optical thickness and higher altitude of cloud layers make them more problematic for OCO data processing. Because cloud is extended, the clear cases are spatially correlated. Assuming that a target A is clear, the probability that target B is clear is

$$P_B = \overline{P} + (1 - \overline{P})F(d) \quad (1)$$

where $\overline{P}$ is the fraction of clear sky for the area and d is the distance between A and B. The function F is unity for zero distance, and is expected to decrease to zero at large distances. This expectation is confirmed by GLAS data, as shown in Figure 5, where F is plotted for 10 degree latitude bands from the north to the south pole. We have analyzed all available GLA11 products and counted the occurrences of clear and cloudy pixel couples (four possible cases) as a function of their distance along the GLAS track. The statistics are therefore valid mostly along the North-South direction. The respective counts of occurrences yields P(B) and P(B|A), i.e. the fraction of clear pixels and the fraction when A is clear. F is then estimated as

$$F = (P(B|A) - P(B))/(1 - P(B)) \quad (2)$$

The decrease of F is monotonic, very rapidly for a few tens of kilometers, but continuing more slowly over several thousand kilometers. A representative spatial scale of the clear areas, denoted d_0 and defined to be the distance at which F falls to $1/e$, is shown in Table 1 for the latitude bands. Zonal variations of d_0 are rather small between 60N and 60S, where the range is only 25% of the mean of approximately 320 km. However, d_0 is significantly shorter at high latitudes in the north but longer in the south. The function F is approximated well by $\exp[-(d/d_0)^{0.5}]$ as shown in Figure 5, but not by $\exp[-d/d_0]$ (not shown). The physical explanation for this functional form presently is unclear, but it is affected both by the size distribution of cloud cells [*Machado and Rossow*, 1993] as well as their shape, which may have fractal properties [*Lovejoy*, 1982]. The presence of small clouds leads to a rapid decrease of the

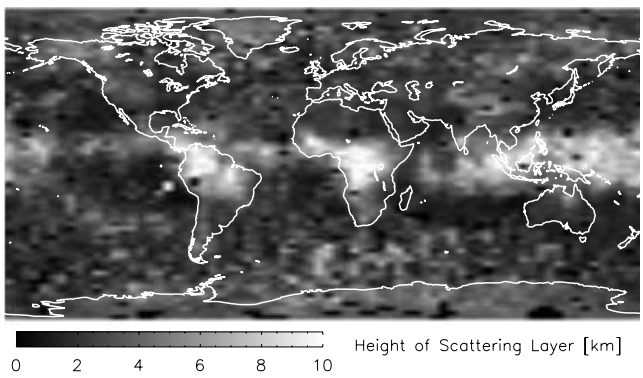

Figure 3. Mean height of the scattering layer for cases with an optical thickness (either cloud or aerosol or both) between 0 (excluded) and 0.2.

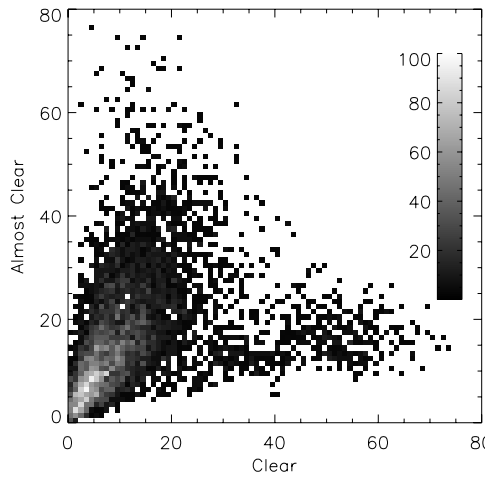

Figure 4. Fraction of almost clear cases (optical thickness less than 0.2) as a function of the number of totally clear cases. This figure is based on the monthly means shown in Figures 1 and 2. The color scale range is arbitrary.

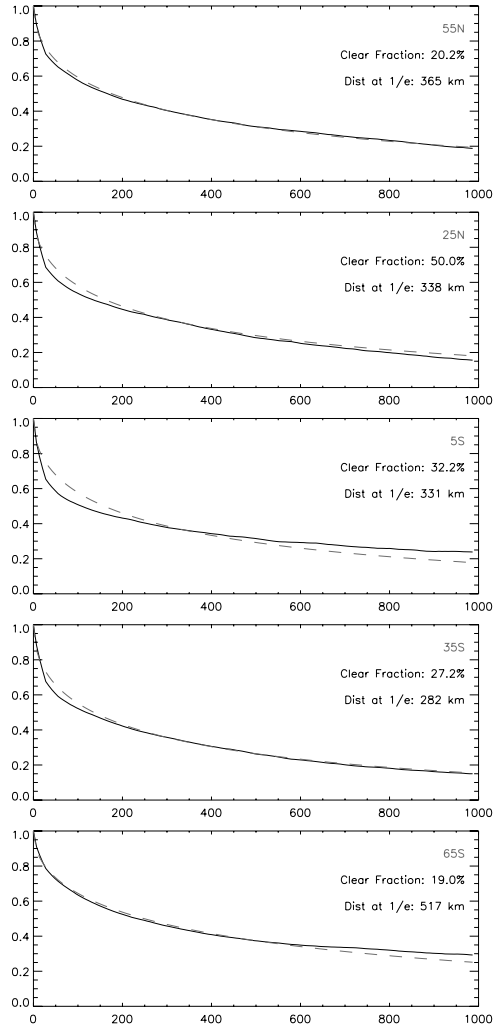

Figure 5. Conditional probability function F (see equation 1) for six latitude bands. The plain line is the experimental data, while the dashed line shows the function $\exp[-(d/d_0)^{0.5}]$, where d_0 is the distance at which the experimental F falls to 1/e.

function at small distance, while large cloud cells can explain the long tail.

4. Discussion and Conclusions

[16] One may question whether the present results are valid for other periods than October. At this point, we do not see evidence of exceptional meteorological or aerosol conditions that would have a global impact in October. Further investigation of this issue must await the release of CALIPSO data in early 2006.

[17] Despite the limited temporal coverage of its available observations, GLAS now provides valuable data on the statistics of scattering layers in the atmosphere, which we have examined in the context of OCO. Atmospheric scattering is below the detection limit of GLAS for approximately 15% of the cases. The best accuracy in OCO products is expected from these cases. A significant fraction (≈20%) of scattering atmospheres have optical thickness less than 0.2 in the visible. Such cases also may yield useful CO_2 estimates, especially as GLAS shows that most correspond to low-level aerosol layers, which have a smaller impact on the OCO spectra than elevated clouds [*O'Brien and Rayner*, 2002]. The global fraction of almost clear atmospheres, i.e. those potentially useful in this context, appears significantly larger than assumed in preparation studies such as in the work by *Rayner et al.* [2002]. The ability to process OCO spectra affected by thin layers of aerosol and cloud would increase the number of retrievals by more than a factor of 2, but it would not change greatly their spatial distribution. Thus, in applications of OCO data where accuracy is essential but the spatial density of data points is not a limiting factor, it might be advisable to use only data from the clearest atmospheres, with neither aerosol nor cloud at the detection limit of GLAS.

[18] **Acknowledgment.** We thank the National Snow and Ice Data Center for distributing the GLAS products and documentation and the ICARE processing center for helping with the analysis of GLAS data.

References

Abshire, J., X. Sun, H. Riris, M. Sirota, J. McGarry, S. Palm, D. Yi, and P. Liiva (2005), Geoscience Laser Altimeter System (GLAS) on the ICESat mission: On-orbit measurement performance, *Geophys. Res. Lett.*, *32,* L21S02, doi:10.1029/2005GL024028.

Crisp, D., et al. (2004), Orbiting Carbon Observatory (OCO) mission, *Adv. Space. Res.*, *34*, 700–709.

Hart, W. D., S. P. Palm, D. L. Hlavka, and J. D. Spinhirne (2005), Lidar global cloud and aerosol layer distribution statistics from GLAS observations, paper presented at AMS Symposium on Lidar Atmospheric Applications, Am. Meteorol. Soc., San Diego, Calif.

Hlavka, D. L., S. P. Palm, W. D. Hart, J. D. Spinhirne, M. J. McGill, and E. J. Welton (2005), Aerosol and cloud optical depth from GLAS: Results and verification for an October 2003 California fire smoke case, *Geophys. Res. Lett.*, *32*, L22S07, doi:10.1029/2005GL023413.

Lovejoy, S. (1982), Area-perimeter relation for rain and cloud areas, *Science*, *216*, 185–187.

Machado, L. A. T., and W. B. Rossow (1993), Structural characteristics and radiative properties of tropical cloud clusters, *Mon. Weather Rev.*, *121*, 3234–3260.

Menzies, R. T., D. M. Tratt, J. D. Spinhirne, and D. L. Hlavka (2002), Aerosol layers over the Pacific Ocean: Vertical distributions and optical properties as observed by multiwavelength airborne lidars, *J. Geophys. Res.*, *107*(D16), 4292, doi:10.1029/2001JD001196.

O'Brien, D. M., and P. J. Rayner (2002), Global observations of the carbon budget: 2. CO_2 column from differential absorption of reflected sunlight in the 1.61 μm band of CO_2, *J. Geophys. Res.*, *107*(D18), 4354, doi:10.1029/2001JD000617.

Palm, S. P., W. D. Hart, D. L. Hlavka, E. J. Welton, A. Mahesh, and J. D. Spinhirne (2002), GLAS Atmospheric Data Products, Geoscience Laser Altimeter System (GLAS) algorithm theoretical basis document, version 4.2, 137 pp., Goddard Space Flight Cent., Greenbelt, Md.

Rayner, P. J., R. M. Law, D. M. O'Brien, T. M. Butler, and A. C. Dilley (2002), Global observations of the carbon budget: 3. Initial assessment of the impact of satellite orbit, scan geometry, and cloud on measuring CO_2 from space, *J. Geophys. Res.*, *107*(D21), 4557, doi:10.1029/2001JD000618.

Spinhirne, J. D., S. P. Palm, W. D. Hart, D. L. Hlavka, and E. J. Welton (2005), Cloud and aerosol measurements from GLAS: Overview and initial results, *Geophys. Res. Lett.*, *32*, L22S03, doi:10.1029/2005GL023507.

Zwally, H. J., R. Schutz, S. Palm, W. Hart, D. L. Hlavka, J. D. Spinhirne, and E. J. Welton (2004), GLAS/ICESat L1B global backscatter data V019 (December 2004), Natl. Snow and Ice Data Cent., Boulder, Colo.

F. M. Bréon, Laboratoire des Sciences du Climat et de l'Environnement, CEA/DSM/LSCE, F-91191 Gif sur Yvette, France. (fmbreon@cea.fr)

D. M. O'Brien, Atmospheric Science Department, Colorado State University, Fort Collins, CO 80523, USA.

J. D. Spinhirne, NASA Goddard Space Flight Center/613.1, Greenbelt, MD 20771, USA.